# Snow density along the route traversed by the Japanese–Swedish Antarctic Expedition 2007/08

Shin SUGIYAMA,[1] Hiroyuki ENOMOTO,[2] Shuji FUJITA,[2] Kotaro FUKUI,[3] Fumio NAKAZAWA,[2] Per HOLMLUND,[4] Sylviane SURDYK[2]

[1]*Institute of Low Temperature Science, Hokkaido University, Sapporo, Japan*
*E-mail: sugishin@lowtem.hokudai.ac.jp*
[2]*National Institute of Polar Research, Tachikawa, Japan*
[3]*Tateyama Caldera Sabo Museum, Toyama, Japan*
[4]*Department of Physical Geography and Quaternary Geology, Stockholm University, Stockholm, Sweden*

**ABSTRACT. During the Japanese–Swedish Antarctic traverse expedition of 2007/08, we measured the surface snow density at 46 locations along the 2800 km long route from Syowa station to Wasa station in East Antarctica. The mean snow density for the upper 1 (or 0.5) m layer varied from 333 to 439 kg m$^{-3}$ over a region spanning an elevation range of 365–3800 m a.s.l. The density variations were associated with the elevation of the sampling sites; the density decreased as the elevation increased, moving from the coastal region inland. However, the density was relatively insensitive to the change in elevation along the ridge on the Antarctic plateau between Dome F and Kohnen stations. Because surface wind is weak in this region, irrespective of elevation, the wind speed was suggested to play a key role in the near-surface densification. The results of multiple regression performed on the density using meteorological variables were significantly improved by the inclusion of wind speed as a predictor. The regression analysis yielded a linear dependence between the density and the wind speed, with a coefficient of 13.5 kg m$^{-3}$ (m s$^{-1}$)$^{-1}$. This relationship is nearly three times stronger than a value previously computed from a dataset available in Antarctica. Our data indicate that the wind speed is more important to estimates of the surface snow density in Antarctica than has been previously assumed.**

## 1. INTRODUCTION

Knowledge of the near-surface snow density is essential for the study of surface processes in the Antarctic ice sheet. For instance, the snow density is required to calculate the surface mass balance from stake measurements (e.g. Hubbard and Glasser, 2005; Takahashi and Kameda, 2007) and to interpret satellite/airborne altimetry (e.g. Zwally and Li, 2002; Helsen and others, 2008). The density is also important for various types of satellite data analyses because it is directly related to the dielectric permittivity of snow (e.g. Tiuri and others, 1984), which controls the emission and reflection of electromagnetic waves (e.g. Grody, 2008; Lacroix and others, 2009). Further, snow densification accompanies changes in the size, structure and bonding of snow particles, properties which are important for finding climatic signals in deep ice cores.

With these factors as motivation, surface snow density and the densification process have been studied by numerous observational (field and satellite), theoretical and numerical methods. The snow density has been measured at many locations in Antarctica (e.g. Cameron and others, 1968; Endo and Fujiwara, 1973; Braaten, 1997; Oerter and others, 1999; Eisen and others, 2008; Kameda and others, 2008). Near-surface densification processes have been studied by measuring the vertical density profiles of firn cores and shallow pits (e.g. Alley, 1988; Craven and Allison, 1998; Van den Broeke and others, 1999; Fujita and others, 2009; Vihma and others, 2011). These field data have been used to develop and calibrate numerous snow densification models (e.g. Herron and Langway, 1980; Kameda and others, 1994; Spencer and others, 2001).

Since the direct determination of snow density from satellite data remains difficult, firn-core analyses and pit measurements are the only means to obtain reliable data. However, it is difficult to cover a large area using point measurements, and the measurement sites are not uniformly distributed throughout Antarctica. To overcome these problems, densification models have been coupled with climate and meteorological models to compute the density distribution over the entire ice sheet. Density maps obtained using these models have contributed to our understanding of the age of gases contained in ice cores (Kaspers and others, 2004), firn thickness (Van den Broeke, 2008) and ice-sheet elevation change (Helsen and others, 2008). Such an approach requires an accurate densification model calibrated with field data, and the modeled density map needs to be validated through comparison with field observations.

Despite the need for reliable near-surface snow density data, previously reported field measurements are insufficient to cover the large variability in meteorological and geometrical conditions in Antarctica. Data are particularly scarce for the interior of the ice sheet. To contribute to our understanding of the snow density distribution and densification processes in Antarctica, we carried out shallow pit measurements during the Japanese–Swedish traverse expedition in the 2007/08 austral summer. In this paper, we report upper 1 (or 0.5) m density profiles collected at 46 survey sites, from coastal to inland plateau areas in East Antarctica. The influence of meteorological variables on near-surface densification is discussed in light of the density variation measured along the 2800 km long route.

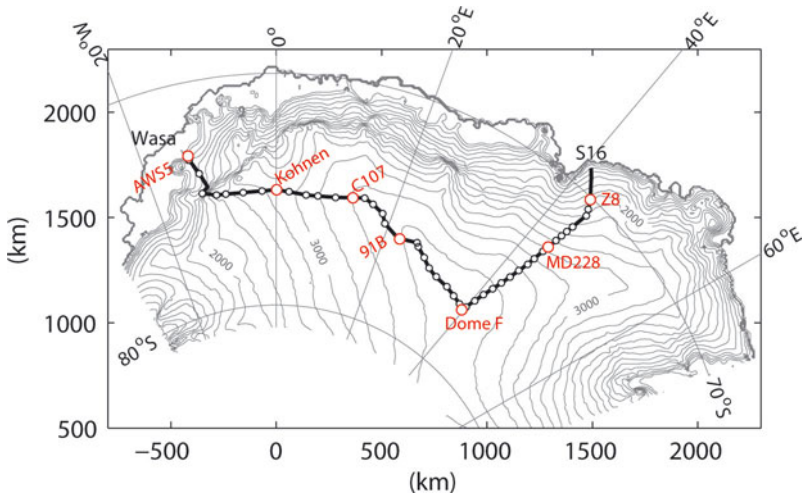


**Fig. 1.** Map of the study region, along with the route traversed by the Japanese–Swedish Antarctic Expedition in 2007/08. Open circles denote the locations of snow-pit measurements. Red circles denote measurement sites referred to in the text. The contours represent surface elevation at intervals of 200 m, based on Bamber and others (2009).

## 2. METHOD

### 2.1. Study site

From November 2007 to January 2008, Japanese and Swedish research teams carried out a traverse expedition in East Antarctica, between the Japanese inland base S16 (30 km from Syowa station; 69.03° S, 40.05° E; 589 m a.s.l.) and the Swedish Wasa station (73.05° S, 13.37° W; 292 m a.s.l.) (Fig. 1; Table 1) (Holmlund and Fujita, 2009). The two teams departed from their home stations in snow vehicles and met at a point ~1400 km from each of the starting points (75.89° S, 25.83° E; 3661 m a.s.l.). They exchanged some expedition members and scientific instruments before they began their return trips. Accordingly, various research activities could be carried out along the entire stretch from S16 to Wasa (Sugiyama and others, 2010; Fujita and others, 2011).

During the expedition, we measured the density, grain size and structure of snow in the near-surface layer at 46 locations along the route (to 1 m depth at 35 locations and to 0.5 m at 11 locations) (Fig. 1). The first survey was made at Z8 (180 km inland from S16) on 17 November 2007. The snow survey was repeated along the rest of the expedition route (covering >2650 km), with measurements taken at intervals of approximately 20–100 km until the final measurement was completed at AWS5 near Wasa station, on 28 January 2008. The elevation of the measurement sites increased from 1991 m (Z8) to 3800 m (Dome F), then gradually decreased to 2500 m at the point 290 km west of Kohnen station. From this point, the route descended steeply from the Antarctic plateau to the coastal region. Annual snow layer thicknesses near the surface have previously been measured at 50–400 mm for the section between Z8 and Dome F (Furukawa and others, 1996), 140–250 mm in the vicinity of Kohnen (Oerter and others, 1999) and 550 ± 110 mm for the coastal region near Wasa (Kärkäs and others, 2005). The uppermost 1 m of snow cover therefore consists of several annual layers, in some cases more than ten.

**Table 1.** Sites along the expedition route referred to in the text

| Site | Lat. | Long. | Elevation | Distance from S16 |
|---|---|---|---|---|
| | | | m | km |
| S16 | 69.03° S | 40.05° E | 589 | 0 |
| Z8 | 70.08° S | 43.24° E | 1991 | 180 |
| MD228 | 72.79° S | 43.52° E | 2960 | 495 |
| Dome F | 77.32° S | 39.70° E | 3800 | 1006 |
| 91B | 76.05° S | 22.74° E | 3595 | 1497 |
| C107 | 74.97° S | 12.89° E | 3424 | 1831 |
| Kohnen | 75.00° S | 0.01° E | 2890 | 2202 |
| AWS5 | 73.11° S | 13.17° W | 365 | 2823 |

### 2.2. Measurements

Snow measurements were performed on a side-wall of a snow pit excavated at each survey site. We measured the density by sampling a 30 mm thick snow block using a box-type stainless density cutter (30 mm × 60 mm × 56 mm, Climate Engineering Co.). A digital bench scale (CS200, OHAUS Co.) with a resolution of ±0.1 g was used to weigh the snow blocks. This error corresponds to <1% of measured weight. The accuracy for density measurements performed with similar devices and procedures has been reported as ±4% (Conger and McClung, 2009). The sampling was performed from the surface to 1 (or 0.5) m depth, at intervals of 30 mm.

Stratigraphical information was recorded following the guidelines given by Colbeck and others (1990). We identified layers after a visual inspection of the snow structure and grain size. The snow structure was classified into four types: fresh snow; compacted snow (Fig. 2a); faceted crystals or depth hoar (we refer to both types of structure as depth hoar in the remainder of this paper) (Fig. 2b); and a crust layer (Fig. 2c). The compacted snow layers include those compacted under overburden stress as well as wind compaction. The crust layers are less than several millimeters thick well-bonded snow, formed probably at the surface due to radiation or wind. The grain size was measured using a magnifier on a plastic plate ruled in millimeters. Several snow samples were taken from each stratigraphic layer, to allow precise measurement of the

average grain size. The permittivity of snow was also measured using a snow fork (a parallel-wire transmission-line resonator), whose results are presented elsewhere (Sugiyama and others, 2010).

## 3. RESULTS

Figure 3 shows vertical profiles of snow density, grain size and the four structures obtained at six selected locations as typical examples of the data. At MD228 (2960 m a.s.l.; 495 km from S16), on the slope ascending from S16 to Dome F, the snow was relatively dense (mean density 425 kg m$^{-3}$), fine-grained (mean grain size 0.33 mm) and dominated by a compacted snow structure (Fig. 3a). At the measurement sites located inland (Dome F, 91B, C107 and Kohnen), the snow was characterized by depth-hoar structures consisting of medium (0.5–1.0 mm) to coarse (1.0–2.0 mm) grains (Fig. 3b–e). The grain size increased with depth in the pits. Several compacted snow layers were scattered in the snowpack, forming relatively dense and fine-grained layers. At C107, for example, there were three compacted snow layers at depth ranges of 0.17–0.35, 0.40–0.42 and 0.81–0.96 m from the surface. All three layers were dense and fine-grained (Fig. 3d). Some of these were exceptionally hard and dense, with tightly bound fine snow grains (0.2–0.5 mm) (Fig. 2a). Crust layers several millimeters thick were frequently observed in this region (Fig. 2c). In the coastal region near Wasa station (AWS5), the snow properties were similar to those at MD228 in terms of high density (419 kg m$^{-3}$) and domination by compacted snow (Fig. 3f).

Figure 4 displays vertical profiles of snow density, grain size and stratification obtained over the traverse route. The plot shows an inhomogeneous distribution of snow properties in the horizontal and vertical directions. In general, the density decreased from the coastal region towards Dome F, and increased from Kohnen to Wasa (Fig. 4a). However, a given density profile obtained at one site was not necessarily similar to those obtained at nearby sites. For example, very high-density layers (>500 kg m$^{-3}$) were observed in a few inland profiles (1000–2000 km from S16), but vertical positions of the layers do not correspond. Thus, it was very difficult to define a characteristic high- or low-density layer that could be interpreted as an isochrone.

The grain size generally increased with distance from the surface (Fig. 4b). Grains were <0.5 mm near the surface, but ranged from 1.0 to 3.0 mm at depths of 1 m. Inland snow was more dominated by depth-hoar structures, while compacted snow structure accounted for a larger proportion near the coast (Fig. 4c). As observed in the density data, neighboring stratifications did not correspond with each other. The vertical positions of compacted snow layers and crust layers were not continuously distributed in the horizontal direction.

The mean density variations along the route showed interesting features when compared with the surface elevation (Fig. 5a and b). On the route ascending from Z8 to Dome F, the mean density was relatively constant until around MD228, with values in the range 403–439 kg m$^{-3}$. After MD228, we observed a marked decrease in mean density as we approached Dome F. This density decrease at ~3000 m a.s.l. has been reported in previous measurements performed along the same route (Endo and Fujiwara, 1973; Yamada and Watanabe, 1978; Shiraiwa and others, 1996). The decrease in density is not consistent with the steadily increasing surface elevation along this section. The mean density was nearly constant from Dome F to Kohnen, with values ranging from 333 to 375 kg m$^{-3}$, whereas the elevation drops from 3800 to 2890 m. The overall mean density between Dome F and Kohnen was 351 kg m$^{-3}$, 17% lower than the mean density between Z8 and MD228 (421 kg m$^{-3}$). The density increased from Kohnen towards the margin of the Antarctic plateau, and exceeded 400 kg m$^{-3}$ after the steep descent from the plateau to the coastal region. Similar density variations have previously been reported in this region (Van den Broeke and others, 1999).

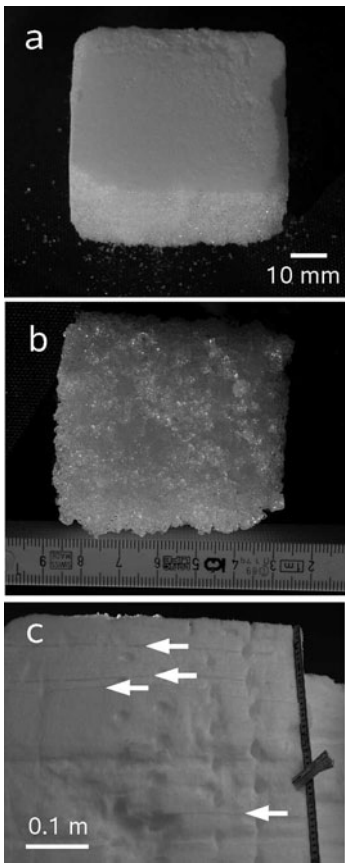


**Fig. 2.** Photographs of characteristic snow structures: (a) very hard compacted snow, (b) depth hoar and (c) crust layers indicated by the arrows.

The changes in grain size and snow structure in the vicinity of Dome F corresponded with the density variations. The grain size increased from MD228 to Dome F, then remained fairly steady between Dome F and Kohnen (Fig. 5c). This change can be seen by comparing the regression lines obtained for the two sections. Similarly, the proportion of compacted snow layers decreased from MD228 to Dome F, but was relatively constant between Dome F and Kohnen (Fig. 5d). In general, the compacted snow-layer proportion varied in a manner similar to the density over the entire traverse route. It was also observed that the number of crust layers increased at around Dome F and remained large until the route descended towards Wasa (Fig. 5e).

## 4. DISCUSSION

### 4.1. Spatial heterogeneity

Within each of the snow pits, individual density measurements showed large variations (Fig. 5b). These signals in the

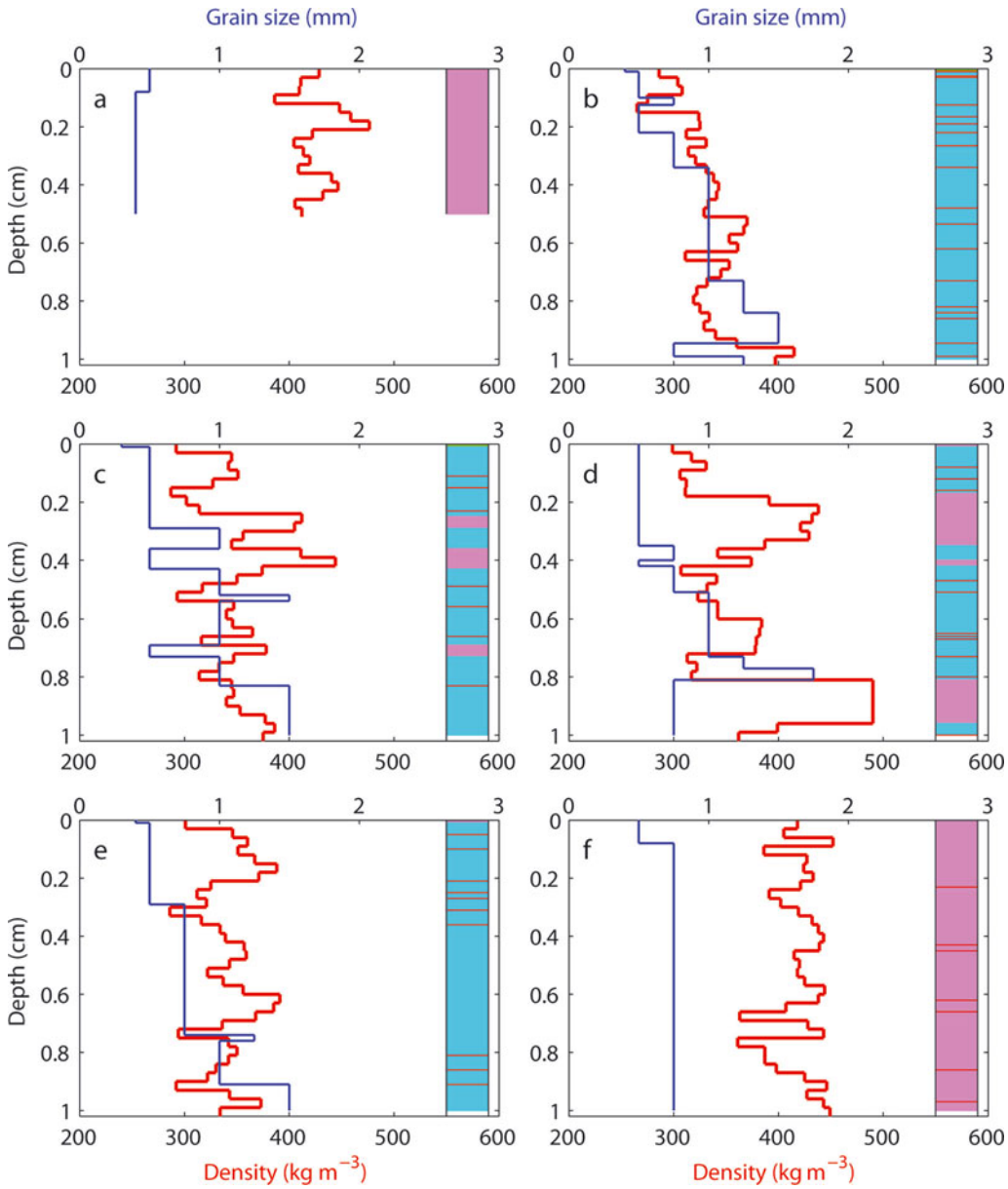


**Fig. 3.** Density (red line), grain size (blue line) and stratigraphy measured at (a) MD228, (b) Dome F, (c) 91B, (d) C107, (e) Kohnen and (f) AWS5 (see Fig. 1 and Table 1 for locations). The snow structures are classified as faceted crystals and depth hoar (magenta), compacted snow (cyan) or a crust layer (red line).

vertical density profiles are often useful to study seasonal/annual variations and events in meteorological conditions. However, the standard deviation of density measurements at each site ranged from 17 to 62 kg m$^{-3}$, with no significant trend along the expedition route (Fig. 5e). The frequency and locations of the high-density layers were not consistent among nearby survey sites. These observations suggest spatial heterogeneity in the depositional processes, on a relatively small scale.

On the scale of 1–10 m, the density profile is influenced by non-uniformly distributed snow surface features such as sastrugi and small-scale dunes (e.g. Watanabe, 1978; Frezzotti and others, 2005). These features are created by wind-driven deposition and erosion. Even when the layering is uniform over a 10 m scale, it is often difficult to cross-correlate layers observed at locations separated by 100 m to several hundred meters (Sturm and Benson, 2004). Depositional conditions are strongly affected by the wind, which is controlled by the ice-sheet surface topography on scales greater than several kilometers (e.g. Furukawa and others, 1996; Frezzotti and others, 2007). Since spatial scales of these variabilities are smaller than the intervals of our pits, it is not straightforward to use the vertical density profiles to understand temporal changes in meteorological and depositional conditions. In the remainder of the paper, we focus our attention on the vertically integrated mean density, and discuss its variations along the route and the role of meteorological conditions in this variable.

### 4.2. Elevation/temperature effect

Changes in the upper 1 (or 0.5) m mean density were associated with changes in the surface elevation along the route (Fig. 5a and b). The mean density decreased as the elevation increased from MD228 to Dome F, but this value changed only a little between Dome F and Kohnen. This is because our route after Dome F followed a ridge with

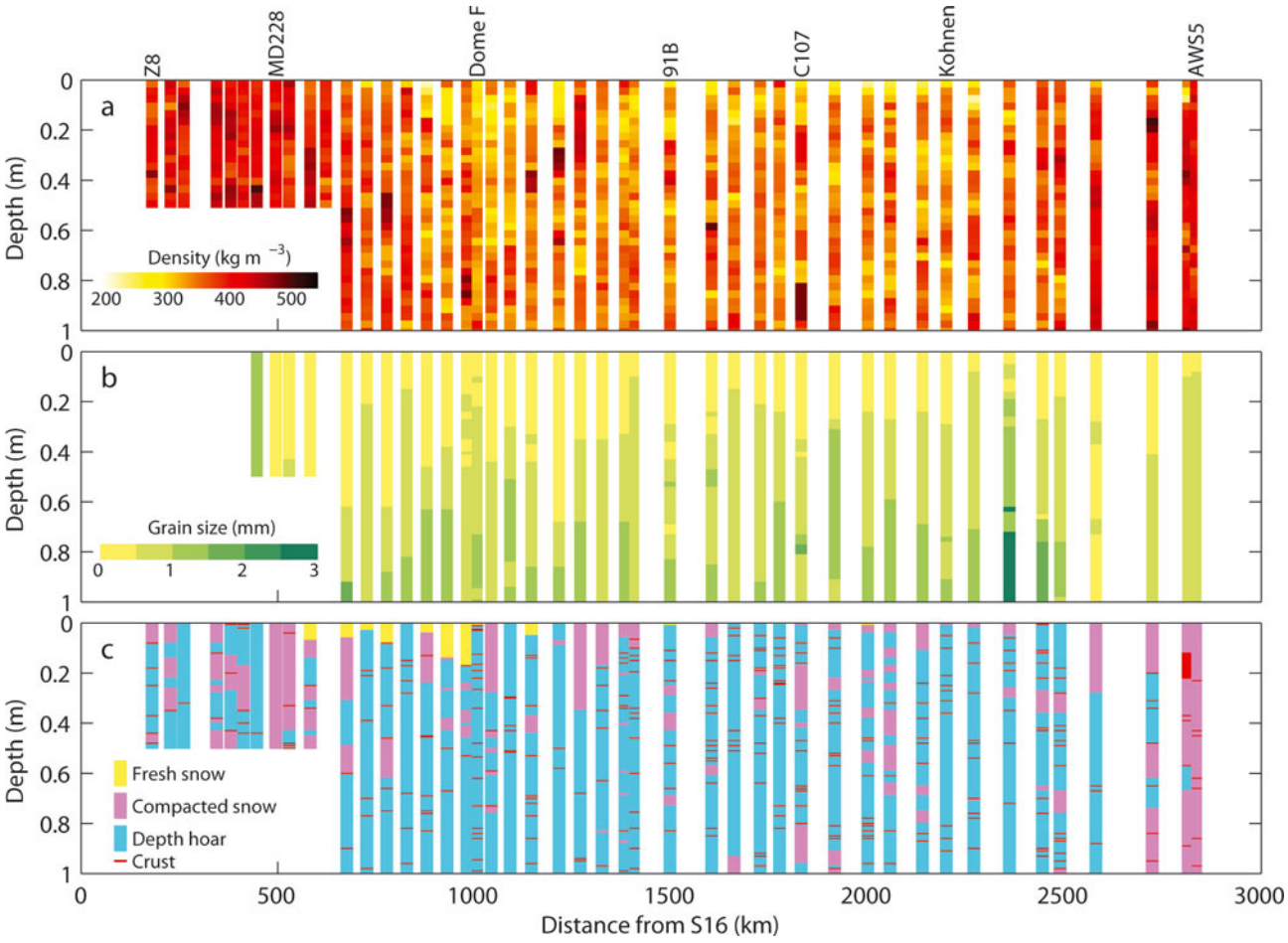


**Fig. 4.** Vertical profiles of (a) snow density, (b) grain size and (c) stratigraphy measured at 46 locations along the expedition route.

relatively constant elevation on the Antarctic plateau (Fig. 1). The density increased again when the route descended from Kohnen to Wasa. Accordingly, we obtain an inverse relationship between the mean density and elevation (Fig. 6a). A likely interpretation of this relationship concerns the surface temperature, which is known to play a key role in snow densification in polar regions (e.g. Herron and Langway, 1980; Kameda and others, 1994; Arthern and Wingham, 1998; Li and Zwally, 2002). Kaspers and others (2004) compiled near-surface snow density data from Antarctica, and found that surface temperature was the meteorological variable that most influenced the density. We obtain essentially the same plot when the density is plotted against the 10 m depth snow temperature (Fig. 6b). The temperatures used here are based on the 10 m depth snow temperature measured at 25 locations during our expedition, and the annual mean air temperatures measured at Dome F (Takahashi and others, 2004) and Kohnen (Van den Broeke and others, 2004). We calculated the temperature at density measurement sites by assuming a piecewise linear relationship between the temperature and surface elevation. That is, the relationships were determined separately for the three sections S16–Dome F, Dome F–Kohnen and Kohnen–Wasa. Also shown in Figure 6a and b are near-surface snow densities previously reported for the locations in Antarctica indicated in Figure 7 (Kaspers and others, 2004, and references therein).

The effect of air temperature on the surface snow density is reasonable, but the relationship between these variables was not simple in our data. It is clear from Figure 6a and b that the forms of the density–elevation/temperature relationships differ along the sections ascending from MD228 to Dome F and descending from Dome F to Wasa. As described in Section 3, the density was relatively insensitive to elevation change from Dome F to Kohnen. This segment of the path generates the hysteresis loop in the density–elevation/temperature plots, and implies that the density variation was significantly influenced by additional variables. For instance, the accumulation rate is as important as the temperature in several densification theories and empirical models (e.g. Herron and Langway, 1980; Kameda and others, 1994; Arthern and Wingham, 1998; Li and Zwally, 2002). Thus, we compared our density data with accumulation rates reported along the route. The accumulation data were obtained using stake measurements for the section between S16 and Dome F (Motoyama and others, 2008), ice and snow radar surveys between Dome F and Kohnen (Fujita and others, 2011) and firn-core studies between Kohnen and Wasa (Rotschky and others, 2007). According to these data, the accumulation rate decreased from S16 to Dome F, and gradually increased towards Kohnen (Fig. 5f). A scatter plot shows good correlation between the density and accumulation rate measured from Z8 to Dome F. Nevertheless, the density was rather insensitive to the accumulation rate increase from Dome F to Kohnen (Fig. 6c). Thus, the accumulation rate does not adequately explain the density variation along this section.

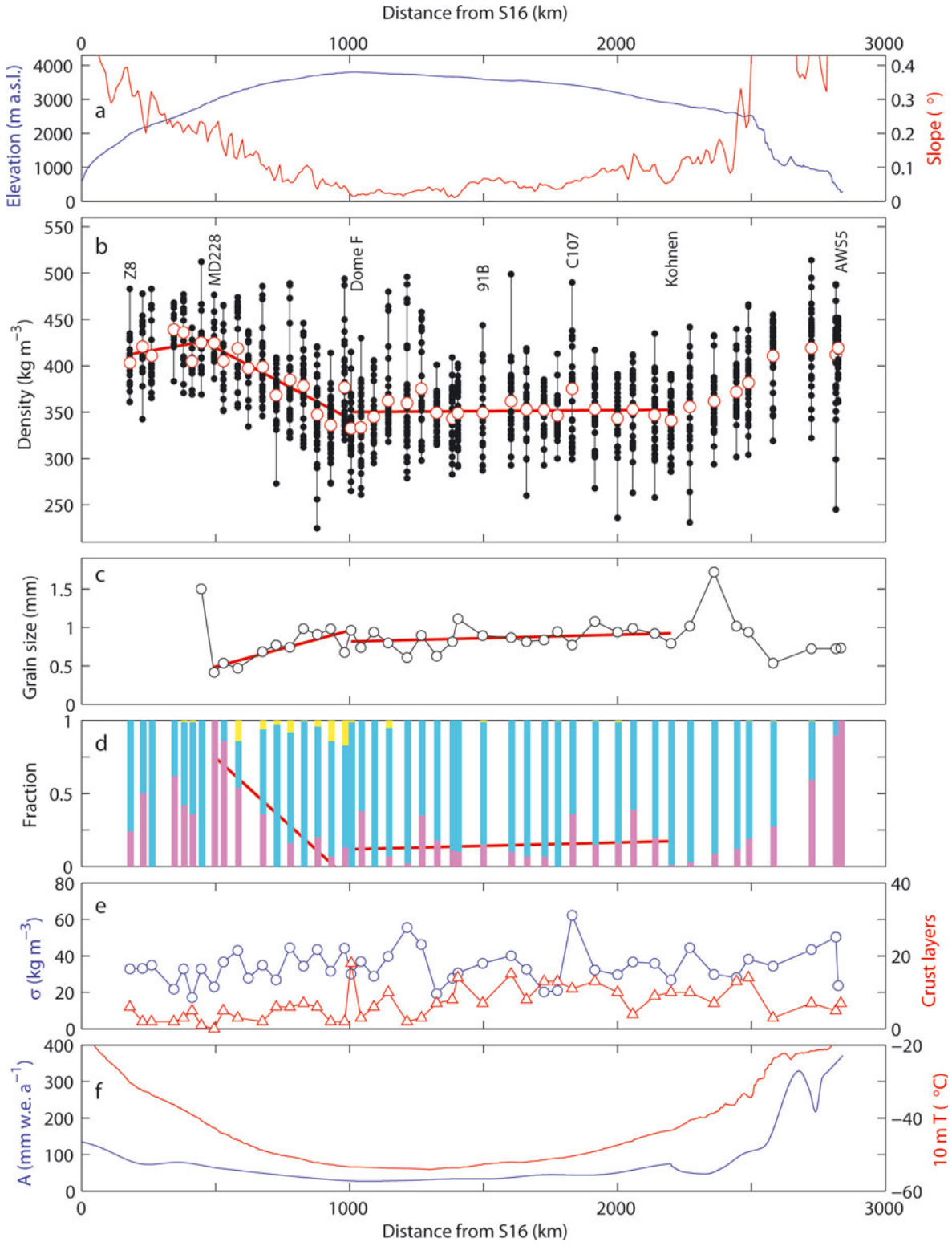


**Fig. 5.** (a) Surface elevation (blue) and slope (red); (b) snow density; (c) grain size; (d) proportion of fresh snow (yellow), depth hoar (cyan) and compacted snow (magenta); (e) standard deviation of density (blue) and frequency of crust layers; and (f) snow accumulation rate (blue) and 10 m depth snow temperature (red) along the expedition route. In (b), individual measurements and mean values are denoted by black dots and red circles respectively. The red lines in (b–d) are linear regressions of the mean density, grain size and the proportion of compacted snow, performed for the sections Z8–MD228, MD228–Dome F and Dome F–Kohnen. The surface slope in (a) was determined using the digital elevation model by Bamber and others (2009).

### 4.3. Wind-speed effect

Another meteorological variable relevant to surficial snow densification is wind speed. The wind-speed pattern over the Antarctic ice sheet is strongly affected by topography, in particular the surface slope (Parish and Bromwich, 1987). Along the expedition route, the surface slope progressively decreased from S16 to Dome F, and was relatively flat thereafter (Fig. 5a). The surface slope and density showed similar variations between MD228 and Kohnen (Fig. 5a and b), suggesting that the wind influenced the densification. In

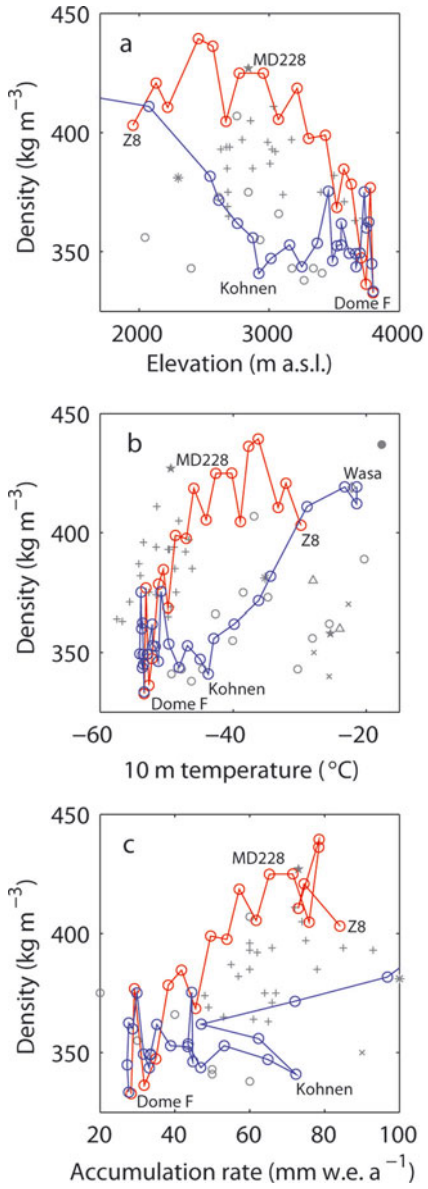


**Fig. 6.** Scatter plots of the density vs (a) surface elevation, (b) 10 m depth snow temperature and (c) accumulation rate. The data obtained in the sections Z8–Dome F and Dome F–Wasa are denoted by red and blue circles respectively. Field data previously reported in Antarctica (Kaspers and others, 2004 and references therein) are indicated by the grey markers in Figure 7.

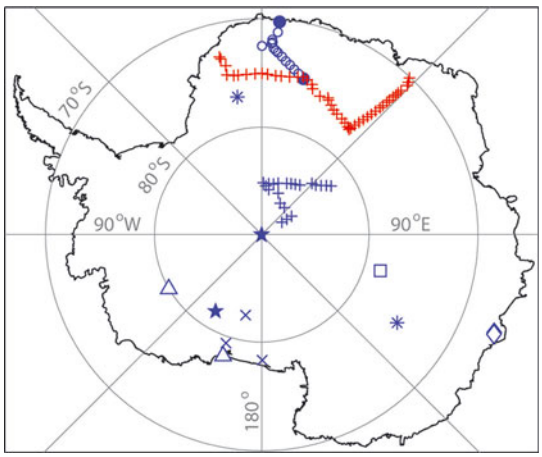


**Fig. 7.** Locations of the snow density measurements in this study (red cross) and previously reported data compiled by Kaspers and others (2004) (blue markers). The sources of the previous data are Kaspers and others (2004) (●); Sturges and others (2001) (∗); Butler and others (1999) (⋆); Trudinger and others (1997) (◇); Bender and others (1994) (□); Gow (1968) (△); Herron and Langway (1980) (×); Van den Broeke and others (1999) (○); and Cameron and others (1968) (+).

Figure 8a, the expedition route is superimposed on a 10 m annual mean wind-speed map generated by a climate model. This map was constructed from the 20 year (1989–2009) averaged output of a regional atmospheric climate model with a horizontal resolution of 27 km (Lenaerts and Van den Broeke, 2012). The computed wind pattern generally represents a topographically controlled katabatic wind system, but also includes the effects of sporadic strong wind events. The first half of the section between S16 and Dome F (the windiest region along our expedition route) was characterized as a strong katabatic wind zone. The wind speed was >8 m s$^{-1}$ from the first measurement site Z8 (180 km from S16) to 128 km inland of MD228 (623 km from S16). The wind speed rapidly decreased inland, reaching a minimum value near Dome F (5.0 m s$^{-1}$). These relatively weak wind conditions extended along the ridge towards Kohnen. The measured density correlated well with the simulated wind speed, with a correlation coefficient $r = 0.79$ (Fig. 8b).

It has been recognized that the wind, as well as temperature, plays a critical role in snow densification in polar regions. Snow grains near the surface are rounded by the wind. This process enhances grain settling and packing, the dominant mechanisms in the initial stage of dry snow densification (e.g. Anderson and Benson, 1963; Herron and Langway, 1980). Strong wind conditions cause moisture transfer within a snowpack, which facilitates wind slab formation over a depth-hoar layer (Benson, 1967). Moreover, snow density is affected by features such as sastrugi, dunes and glazed surfaces, all of which are formed through erosion and deposition processes driven by strong katabatic winds (e.g. Watanabe, 1978). The effects of the wind were also observed in the grain size and snow structure. The grain size increased and the fraction of compacted snow decreased from MD228 to Dome F (Fig. 5c and d). These variations can be explained by the degree of wind compaction, which was expected to decrease towards Dome F.

The influence of wind on surface snow density has been pointed out in previous studies in Antarctica. Based on firn-core analyses at widely spread sampling sites in Antarctica, Craven and Allison (1998) concluded that a 5 m s$^{-1}$ wind-speed increase and a 10°C temperature increase have equivalent effects on the density. Relying on the relationships between snow density and meteorological variables derived by Craven and Allison (1998), Van den Broeke and others (1999) reconstructed a wind-speed pattern from firn density profiles in Dronning Maud Land. According to their analysis, the density at 1 m depth should increase by 8 kg m$^{-3}$ for each wind-speed increase of 1 m s$^{-1}$. This ratio is approximately half the value observed in this study (16.0 kg m$^{-3}$ for every 1 m s$^{-1}$) (Fig. 8b). In addition to the studies just cited, rapid density increases during sporadic strong wind events have been reported in the interior of the ice sheet (Lacroix and others, 2009; Birnbaum and others, 2010).

At the four measurement sites located within 220 km of Wasa station, the density data deviated from the linear

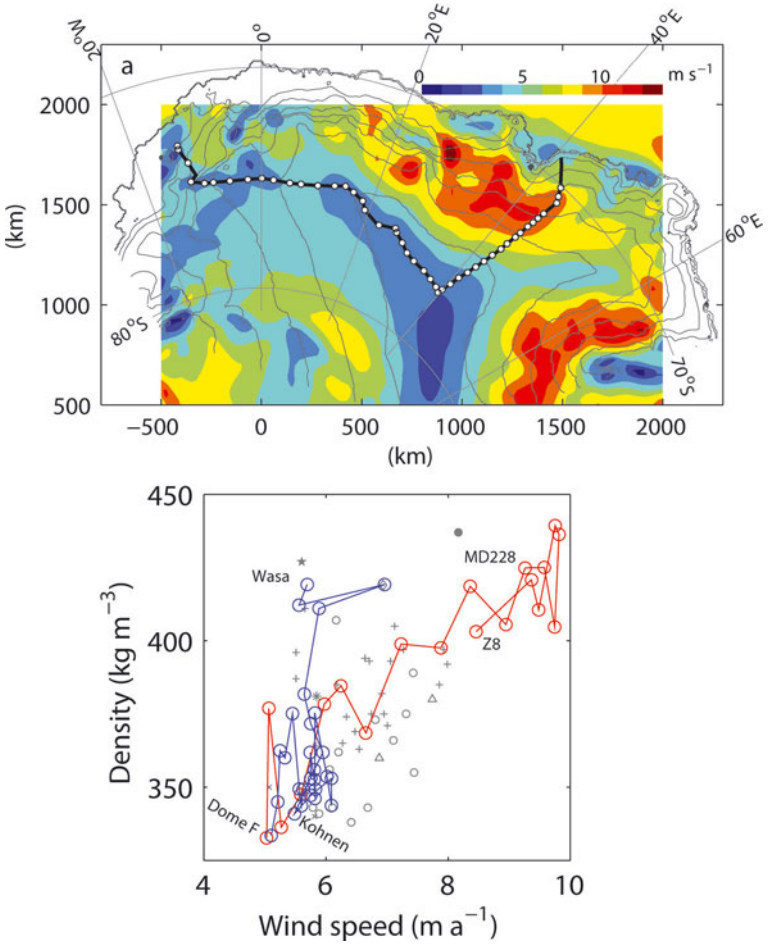


**Fig. 8.** (a) Locations of snow-pit measurements superimposed on a contour map showing 10 m wind-speed distributions. The wind-speed map represents the 20 year (1989–2009) averaged output of a regional atmospheric climate model (Lenaerts and Van den Broeke, 2012). (b) Scatter plot of the density vs the wind speed. Markers are as in Figures 6 and 7.

relationship with wind speed (Fig. 8b). These sites were located at low elevation, near the coast (Fig. 5a and b). A plausible reason for their difference could be that temperatures and accumulation rates are higher near the coast. Another possible interpretation is that sporadic wind events occur more frequently in coastal regions, enhancing the densification. Such short-term events would affect the annual mean wind speed only a little.

### 4.4. Parameterization

Kaspers and others (2004) proposed the following parameterization of surface snow density $\rho_0$ with respect to meteorological variables:

$$\rho_0 = \alpha + \beta T + \delta A + \varepsilon W, \quad (1)$$

where $T$ is the annual mean surface temperature, $A$ is the accumulation rate and $W$ is the annual mean wind speed. They calibrated the parameters $\alpha$, $\beta$, $\delta$ and $\varepsilon$ by fitting the formula to density and meteorological datasets previously obtained at the locations indicated by blue markers in Figure 7 (Kaspers and others, 2004, and references therein). The data used for their calibration included snow density, 10 m depth snow temperature and accumulation rate measured in the field, as well as the 10 m wind speed provided by a regional climate model. Despite the simplicity of this formula, the densities computed using Eqn (1) showed reasonable agreement with the measured values.

We calibrated Eqn (1) using our own snow densities and 10 m depth snow temperatures (this study; Van den Broeke and others, 2004), accumulation rates (Rotschky and others, 2007; Motoyama and others, 2008; Fujita and others, 2011) and annual mean wind speed (Lenaerts and Van den Broeke, 2012), as described earlier in this section and shown in Figures 5f and 8a. Calibration parameters obtained by the least-squares method are listed in Table 2, along with correlation coefficients between the measured and modeled densities. The densities estimated using our own calibration of Eqn (1) correlate well with the field data, as indicated by the blue circles in Figure 9a (correlation coefficient $r = 0.91$, $p < 10^{-6}$ and root-mean-square error $\sigma = 13.1\ \mathrm{kg\,m^{-3}}$). The linear coefficient of wind speed was $\delta = 13.5\ \mathrm{kg\,m^{-3}\,(m\,s^{-1})^{-1}}$, nearly three times greater than the value ($4.77\ \mathrm{kg\,m^{-3}\,(m\,s^{-1})^{-1}}$) reported by Kaspers and others (2004). The regression analysis yielded a very small temperature coefficient ($\beta = 0.543\ \mathrm{kg\,m^{-3}\,°C^{-1}}$), indicating that the contribution of temperature to the density variation was small for the temperature range considered in our analysis ($\Delta T = 32$°C; $\Delta\rho = 17.4\ \mathrm{kg\,m^{-3}}$). The importance of the wind speed was confirmed by a second regression analysis performed omitting the wind-speed term (Table 2). The densities estimated by this model (two variables) deviated more from the measurements ($r = 0.68$; $\sigma = 23.0\ \mathrm{kg\,m^{-3}}$) than the densities determined using Eqn (1) (three variables) (Fig. 9a). Figure 10 shows the performance of both

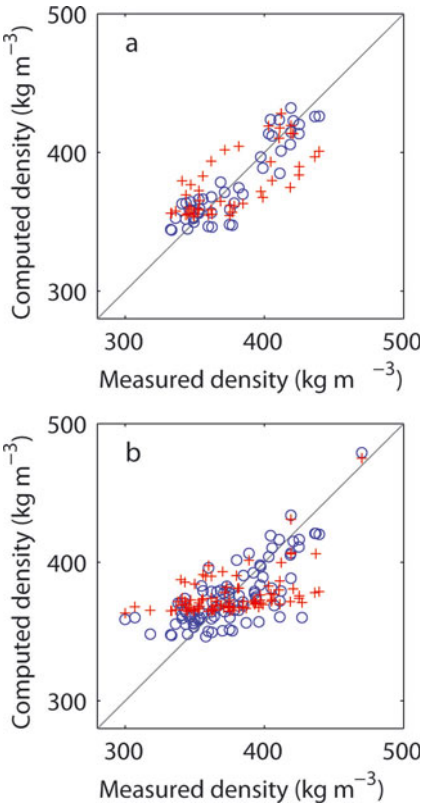


**Fig. 9.** (a) Scatter plot of the densities measured in this study and those estimated from meteorological variables. (b) The same plot, but using a dataset including the densities reported by Kaspers and others (2004). The circles were estimated from the 10 m depth snow temperature, accumulation rate and wind speed. The crosses show estimates from the 10 m depth snow temperatures and accumulation rates only.

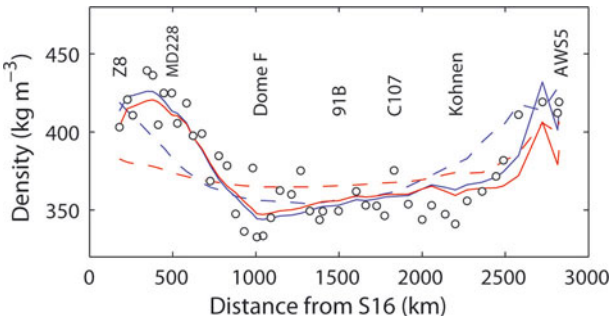


**Fig. 10.** Snow density measured along the traverse route (○) and computed with a linear regression model. The regression coefficients in Eqn (1) were optimized for the data obtained in this study (blue solid line) and for those including previously reported data (blue dashed line). The red lines (solid and dashed) were obtained by omitting the wind-speed term from Eqn (1).

regression analyses. The density variations from the inland plateau to the coastal regions are better reproduced by the model that includes the wind speed. Without the wind speed, the deviation from the observed data increases progressively from Dome F towards Wasa.

The major influence of the wind speed on the surface density was reported by Endo and Fujiwara (1973) in data collected during their traverse expedition from Syowa to the South Pole in 1968/69. The mean density from the surface to 2 m depth correlated well with the surface slope along the route. Using a relationship between the slope and the annual mean wind speed, they derived a linear dependence of the density on the wind speed, with a value of 14 kg m$^{-3}$ (m s$^{-1}$)$^{-1}$. Their coefficient agrees very well with the value obtained in this study. They also found that the density slightly increased as the temperature decreased, within regions where the mean wind speed was less than 10–11 m s$^{-1}$ and the temperature ranged from –60 to –48°C. Endo and Fujiwara (1973) argued that snowflakes are smaller in colder air conditions, which makes the initial snow density after deposition greater. Such an effect should be particularly visible inland, where temperatures and wind speeds are relatively low. A negative dependence of the density on temperature has also been reported in seasonal snow cover in the North American Arctic and Greenland (Bilello, 1967). The small temperature coefficient obtained in our work is consistent with these studies.

We performed additional regression analyses including the density and meteorological data compiled by Kaspers and others (2004). However, the wind speeds in Kaspers' original dataset were replaced with recent modeling results (Lenaerts and Van den Broeke, 2012). The parameters determined for a combined dataset (46 sites from this study and 49 sites compiled by Kaspers and others, 2004) (Fig. 7) are listed in Table 2. The density is more accurately estimated when we include the wind speed as a predictor, as shown in Figure 9b ($r = 0.75$ and $\sigma = 20.7$ kg m$^{-3}$ for the three-variable model, while $r = 0.50$ and $\sigma = 27.1$ kg m$^{-3}$ for the two-variable model). Overall, the performance of the regression model worsened with the inclusion of Kaspers and others' (1994) data (Fig. 10), which were collected from a wide area of Antarctica. It is more difficult to reproduce the clear change in the density from the coastal regions to the inland area. This result implies that the relative importance of the three predictor variables differs significantly in

**Table 2.** Fitting equations, correlation coefficients ($r$), $p$-values and root-mean-square errors ($\sigma$) obtained by multiple regression analysis of the density ($\rho$ in kg m$^{-3}$), 10 m depth snow temperature ($T$ in °C), accumulation rate ($A$ in mm a$^{-1}$) and wind speed ($W$ in m s$^{-1}$), performed with a dataset of size $n$

| Equation | $r$ | $p$ | $\sigma$ kg m$^{-3}$ | $n$ | Data source |
|---|---|---|---|---|---|
| $\rho = 305 + 0.629T + 0.150A + 13.5W$ | 0.91 | $<10^{-6}$ | 13.0 | 46 | This study |
| $\rho = 515 + 2.93T - 0.106A$ | 0.72 | $<10^{-6}$ | 21.8 | 46 | This study |
| $\rho = 284 + 0.170T + 0.0962\ A + 13.8\ W$ | 0.75 | $<10^{-6}$ | 20.7 | 95 | This study and Kaspers and others (2004) |
| $\rho = 392 + 0.555T + 0.0851\ A$ | 0.50 | $<10^{-6}$ | 27.0 | 95 | This study and Kaspers and others (2004) |

these regions, or that additional conditions with an impact on the density are coming into play. Thus, care should be taken when a linear regression model is applied to an extended region influenced by a broader range of meteorological and topographical conditions.

## 5. CONCLUSION

Density, structure and grain size were measured in the near-surface snow layer at 46 locations along the route traversed in the Japanese–Swedish Antarctic Expedition 2007/08. The route spanned two coastal stations in East Antarctica, Syowa and Wasa. Its total length was ~2800 km, and its altitudinal range was 365–3800 m a.s.l. The mean density for the upper 1 (or 0.5) m layer varied from 333 to 439 kg m$^{-3}$. In general, the snow had a lower density at higher elevations and in inland locations; this variation was related to meteorological variations between the coast and inland areas.

The elevation/temperature dependence of the density in the section between Dome F and Kohnen stations was significantly different from that in the section from the coastal region to Dome F. Although the density variation was fairly small from Dome F to Kohnen, the elevation dropped significantly from 3800 to 2890 m a.s.l. The traverse route between these two inland stations followed a ridge on the Antarctic plateau, where the wind speed was expected to be smaller than over other sections of the route. Our density data showed a strong, positive correlation with wind-speed distributions computed using a regional climate model (Lenaerts and Van den Broeke, 2012), suggesting the importance of wind in the near-surface densification in this region. The grain size increased and the fraction of compacted snow decreased as we ascended from the coastal region to Dome F, also supporting the important effect of wind on snow metamorphism. Multiple regression analysis yielded a linear dependence of the density on the wind speed. The coefficient of this relationship is 13.5 kg m$^{-3}$ (m s$^{-1}$)$^{-1}$, nearly three times greater than a previously reported value (Kaspers and others, 2004). The strong influence of the wind on the density is consistent with field measurements by Endo and Fujiwara (1973) during their traverse expedition to the South Pole. We conclude that wind-driven densification is a more important process than has previously been assumed in Antarctica.

## ACKNOWLEDGEMENTS

We thank the members of the Japanese–Swedish Antarctic Expedition 2007/08 for help in the field. The field activity was part of the 48th and 49th Japanese Antarctic Research Expedition, and was supported by the National Institute of Polar Research, Tokyo, and the Swedish Polar Research Secretariat. The wind-speed data, computed using a regional climate model, were kindly provided by J.T.M. Lenaerts and M.R. van den Broeke; we gratefully acknowledge their contribution. The surface elevation and 10 m snow temperature data were provided by the US National Snow and Ice Data Center. We thank two anonymous reviewers for comments on the manuscript, and the scientific editor, P. Bartelt. This study was funded by the Japanese Ministry of Education, Science, Sports and Culture, Grant-in-Aid for Scientific Research (A), 20241007, 2008–2010.

## REFERENCES

Alley RB (1988) Concerning the deposition and diagenesis of strata in polar firn. *J. Glaciol.,* **34**(118), 283–290

Anderson DL and Benson CS (1963) The densification and diagenesis of snow. In Kingery WD ed. *Ice and snow: properties, processes, and applications*. MIT Press, Cambridge, MA, 391–411

Arthern RJ and Wingham DJ (1998) The natural fluctuations of firn densification and their effect on the geodetic determination of ice sheet mass balance. *Climatic Change,* **40**(4), 605–624

Bamber JL, Gomez-Dans JL and Griggs JA (2009) *Antarctic 1 km Digital Elevation Model (DEM) from combined ERS-1 radar and ICESat laser satellite altimetry*. National Snow and Ice Data Center, Boulder, CO. Digital media: http://nsidc.org/data/docs/daac/nsidc0422_antarctic_1km_dem/index.html

Bender M and 6 others (1994) Climatic correlations between Greenland and Antarctica during the past 100,000 years. *Nature,* **373**(6513), 393–394.

Benson CS (1967) Polar regions snow cover. In Oura H ed. *Physics of snow and ice*. Institute of Low Temperature Science, Hokkaido University, Sapporo, 1039–1063

Bilello MA (1967) Relationships between climate and regional variations in snow-cover density in North America. In Oura H ed. *Physics of snow and ice*. Institute of Low Temperature Science, Hokkaido University, Sapporo, 1015–1028

Birnbaum G and 14 others (2010) Strong-wind events and their influence on the formation of snow dunes: observations from Kohnen station, Dronning Maud Land, Antarctica. *J. Glaciol.,* **56**(199), 891–902 (doi: 10.3189/002214310794457272)

Braaten DA (1997) Detailed assessment of snow accumulation in katabatic wind areas of the Ross Ice Shelf, Antarctica. *J. Geophys. Res.,* **102**(D25), 30 047–30 058

Butler JH and 8 others (1999) A record of atmospheric halocarbons during the twentieth century from polar firn air. *Nature,* **399**(6738), 749–755

Cameron RL, Picciotto E, Kane HS and Gliozzi J (1968) Glaciology of the Queen Maud Land traverse, 1964–1965 South Pole – pole of relative inaccessibility. *Inst. Polar Stud. Rep.* 23

Colbeck SC and 7 others (1990) *The international classification for seasonal snow on the ground*. International Commission on Snow and Ice, International Association of Scientific Hydrology, Wallingford, Oxon

Conger SM and McClung DM (2009) Comparison of density cutters for snow profile observations. *J. Glaciol.,* **55**(189), 163–169 (doi: 10.3189/002214309788609038)

Craven M and Allison I (1998) Firnification and the effects of wind-packing on Antarctic snow. *Ann. Glaciol.,* **27**, 239–245

Eisen O and 15 others (2008) Ground-based measurements of spatial and temporal variability of snow accumulation in East Antarctica. *Rev. Geophys.,* **46**(RG2), RG2001 (doi: 10.1029/2006RG000218)

Endo Y and Fujiwara K (1973) Characteristics of the snow cover in East Antarctica along the route of the JARE South Pole traverse and factors controlling such characteristics. *JARE Sci. Rep.* 7, 1–27

Frezzotti M and 13 others (2005) Spatial and temporal variability of snow accumulation in East Antarctica from traverse data. *J. Glaciol.,* **51**(172), 113–124 (doi: 10.3189/172756505781829502)

Frezzotti M, Urbini S, Proposito M, Scarchilli C and Gandolfi S (2007) Spatial and temporal variability of surface mass balance near Talos Dome, East Antarctica. *J. Geophys. Res.,* **112**(F2), F02032 (doi: 10.1029/2006JF000638)

Fujita S, Okuyama J, Hori A and Hondoh T (2009) Metamorphism of stratified firn at Dome Fuji, Antarctica: a mechanism for local insolation modulation of gas transport conditions during bubble close off. *J. Geophys. Res.,* **114**(F3), F03023 (doi: 10.1029/2008JF001143)

Fujita S and 25 others (2011) Spatial and temporal variability of snow accumulation rate on East Antarctic divide between ice Dome Fuji and EPICA DML. *Cryosphere*, **5**(4), 1057–1081 (doi: 10.5194/tc-5-1057-2011)

Furukawa T, Kamiyama K and Maeno H (1996) Snow surface features along the traverse route from the coast to Dome Fuji Station, Queen Maud Land, Antarctica. *Proc. NIPR Symp. Polar Meteorol. Glaciol.,* **10**, 13–24

Gow AJ (1968) Deep core studies of the accumulation and densification of snow at Byrd Station and Little America V. *CRREL Res. Rep.* 197

Grody N (2008) Relationship between snow parameters and microwave satellite measurements: theory compared with Advanced Microwave Sounding Unit observations from 23 to 150 GHz. *J. Geophys. Res.,* **113**(D22), D22108 (doi: 10.1029/2007JD009685)

Helsen MM and 7 others (2008) Elevation changes in Antarctica mainly determined by accumulation variability. *Science,* **320**(5883), 1626–1629 (doi: 10.1126/science.1153894)

Herron MM and Langway CC, Jr (1980) Firn densification: an empirical model. *J. Glaciol.,* **25**(93), 373–385

Holmlund P and Fujita S (2009) Japanese–Swedish Antarctic Expedition, JASE. In Thorén A ed. *Swedish Polar Secretariat Year Book 2008*. Swedish Polar Research Secretariat, Stockholm, 18–21

Hubbard B and Glasser N (2005) *Field techniques in glaciology and glacial geomorphology*. Wiley, New York

Kameda T, Shoji H, Kawada K, Watanabe O and Clausen HB (1994) An empirical relation between overburden pressure and firn density. *Ann. Glaciol.,* **20**, 87–94

Kameda T, Motoyama H, Fujita S and Takahashi S (2008) Temporal and spatial variability of surface mass balance at Dome Fuji, East Antarctica, by the stake method from 1995 to 2006. *J. Glaciol.,* **54**(184), 107–116 (doi: 10.3189/002214308784409062)

Kärkäs E, Martma T and Sonninen E (2005) Physical properties and stratigraphy of surface snow in western Dronning Maud Land, Antarctica. *Polar Res.,* **24**(1–2), 55–67 (doi: 10.1111/j.1751-8369.2005.tb00140.x)

Kaspers KA, Van de Wal RSW, Van den Broeke MR, Schwander J, Van Lipzig NPM and Brenninkmeijer CAM (2004) Model calculations of the age of firn air across the Antarctic continent. *Atmos. Chem. Phys.,* **4**(5), 1365–1380 (doi: 10.5194/acp-4-1365-2004)

Lacroix P, Legrésy B, Rémy F, Blarel F, Picard G and Brucker L (2009) Rapid change of snow surface properties at Vostok, East Antarctica, revealed by altimetry and radiometry. *Remote Sens. Environ.,* **113**(12), 2633–2641 (doi: 10.1016/j.rse.2009.07.019)

Lenaerts JTM and Van den Broeke MR (2012) Modeliing drift snow in Antarctica with a regional climate model. 2. Results. *J. Geophys. Res.*, **117**(D5), D05109 (doi: 10.1029/2010JD015419)

Li J and Zwally HJ (2002) Modeled seasonal variations of firn density induced by steady-state surface air-temperature cycle. *Ann. Glaciol.,* **34**, 299–302 (doi: 10.3189/172756402781817707)

Motoyama H, Furukawa T and Nishio F (2008) Study of ice flow observations in Shirase drainage basin and around Dome Fuji area, East Antarctica, by differential GPS method. *Antarct. Rec.,* **52**, 216–231 [In Japanese with English summary]

Oerter H, Graf W, Wilhelms F, Minikin A and Miller H (1999) Accumulation studies on Amundsenisen, Dronning Maud Land, by means of tritium, dielectric profiling and stable-isotope measurements: first results from the 1995–96 and 1996–97 field seasons. *Ann. Glaciol.,* **29**, 1–9 (doi: 10.3189/172756499781820914)

Parish TR and Bromwich DH (1987) The surface windfield over the Antarctic ice sheets. *Nature,* **328**(6125), 51–54

Rotschky G and 6 others (2007) A new surface accumulation map for western Dronning Maud Land, Antarctica, from interpolation of point measurements. *J. Glaciol.,* **53**(182), 385–398 (doi: 10.3189/002214307783258459)

Shiraiwa T, Shoji H, Saito T, Yokoyama K and Watanabe O (1996) Structure and dielectric properties of surface snow along the traverse route from coast to Dome Fuji Station, Queen Maud Land, Antarctica. *Proc. NIPR Symp. Polar Meteorol. Glaciol.,* **10**, 1–12

Spencer MK, Alley RB and Creyts TT (2001) Preliminary firn-densification model with 38-site dataset. *J. Glaciol.,* **47**(159), 671–676 (doi: 10.3189/172756501781831765)

Sturges WT and 7 others (2001) Methyl bromide, other brominated methanes, and methyl iodide in polar firn air. *J. Geophys. Res.*, **106**(D2), 1595–1606

Sturm M and Benson C (2004) Scales of spatial heterogeneity for perennial and seasonal snow layers. *Ann. Glaciol.,* **38**, 253–260 (doi: 10.3189/172756404781815112)

Sugiyama S, Enomoto H, Fujita S, Fukui K, Nakazawa F and Holmlund P (2010) Dielectric permittivity of snow measured along the route traversed in the Japanese–Swedish Antarctic Expedition 2007/08. *Ann. Glaciol.,* **51**(55), 9–15 (doi: 10.3189/172756410791392745)

Takahashi S and Kameda T (2007) Snow density for measuring surface mass balance using the stake method. *J. Glaciol.,* **53**(183), 677–680

Takahashi S, Kameda T, Enomoto H, Motoyama H and Watanabe O (2004) Automatic weather station (AWS) data collected by the 33rd to 42nd Japanese Antarctic Research Expeditions during 1993–2001. *JARE Data Rep.* 276.

Tiuri MT, Sihvola AH, Nyfors EG and Hallikainen MT (1984) The complex dielectric constant of snow at microwave frequencies. *IEEE J. Ocean. Eng.,* **9**(5), 377–382

Trudinger C, Enting IG, Etheridge DM, Francey RJ, Levchenko VA and Steele LP (1997) Modeling air movement and bubble trapping in firn. *J. Geophys. Res.*, **102**(D6), 6747–6763

Van den Broeke M (2008) Depth and density of the Antarctic firn layer. *Arct. Antarct. Alp. Res.,* **40**(2), 432–438

Van den Broeke MR and 6 others (1999) Climate variables along a traverse line in Dronning Maud Land, East Antarctica. *J. Glaciol.,* **45**(150), 295–302

Van den Broeke MR, Van As D, Reijmer CH and Van de Wal RSW (2004) The surface radiation balance in Antarctica as measured with automatic weather stations. *J. Geophys. Res.,* **109**(D9), D09103 (doi: 10.1029/2003JD004394)

Vihma T, Mattila O-P, Pirazzini R and Johansson MM (2011) Spatial and temporal variability in summer snow pack in Dronning Maud Land, Antarctica. *Cryosphere,* **5**(1), 187–201 (doi: 10.5194/tc-5-187-2011)

Watanabe O (1978) Distribution of surface features of snow cover in Mizuho Plateau. *Mem. Natl Inst. Polar Res.,* Special Issue 7, 154–181

Yamada T and Watanabe O (1978) Estimation of mass input in the Shirase and the Soya drainage basins in Mizuho Plateau. *Mem. Natl Inst. Polar Res.,* Special Issue 7, 182–197

Zwally HJ and Li J (2002) Seasonal and interannual variations of firn densification and ice-sheet surface elevation at Greenland summit. *J. Glaciol.,* **48**(161), 199–207 (doi: 10.3189/172756502781831403)

*MS received 23 September 2011 and accepted in revised form 23 January 2012*